Protein Structural Analysis

International Edition: DOI: 10.1002/anie.201809060
German Edition: DOI: 10.1002/ange.201809060

Fast Magic-Angle Spinning ^{19}F NMR Spectroscopy of HIV-1 Capsid Protein Assemblies

Mingzhang Wang[+], Manman Lu[+], Matthew P. Fritz, Caitlin M. Quinn, In-Ja L. Byeon, Chang-Hyeock Byeon, Jochem Struppe, Werner Maas, Angela M. Gronenborn, and Tatyana Polenova**

Abstract: *^{19}F NMR spectroscopy is an attractive and growing area of research with broad applications in biochemistry, chemical biology, medicinal chemistry, and materials science. We have explored fast magic angle spinning (MAS) ^{19}F solid-state NMR spectroscopy in assemblies of HIV-1 capsid protein. Tryptophan residues with fluorine substitution at the 5-position of the indole ring were used as the reporters. The ^{19}F chemical shifts for the five tryptophan residues are distinct, reflecting differences in their local environment. Spin-diffusion and radio-frequency-driven-recoupling experiments were performed at MAS frequencies of 35 kHz and 40–60 kHz, respectively. Fast MAS frequencies of 40–60 kHz are essential for consistently establishing ^{19}F–^{19}F correlations, yielding interatomic distances of the order of 20 Å. Our results demonstrate the potential of fast MAS ^{19}F NMR spectroscopy for structural analysis in large biological assemblies.*

Protein structure determination by magic-angle spinning (MAS) NMR spectroscopy relies largely on experimental interatomic distance constraints. These interatomic distance constraints are extracted from ^{13}C-, ^{15}N-, and ^{1}H-based correlations, which yield distances of up to 6–8 Å.[1–4] Although this approach has been successfully employed to derive the structures of a number of proteins,[5–12] additional information is generally required to determine the quaternary structure or supramolecular organization of multidomain proteins and protein assemblies. ^{19}F MAS NMR spectroscopy is an attractive alternative way of investigating biological systems. ^{19}F is a spin 1/2 nucleus with a very high gyromagnetic ratio and 100% natural abundance, and exhibits a large chemical-shift range (> 300 ppm). The strong ^{19}F–^{19}F dipolar couplings make fluorine well-suited as a long-range distance probe in the solid state, and correlations for distances up to 20 Å have been detected.[13,14] Fluorine is absent from any naturally occurring biological molecule, yet it can be readily and selectively incorporated into proteins,[15–17] largely without causing major structural perturbations.[18] ^{19}F NMR spectroscopy, both solution and solid-state, has therefore emerged as an essential method with broad applications in pharmaceutical chemistry (~30% of all drugs at present in the clinic contain fluorine),[19] chemical biology,[20] biochemistry,[16,21–24] and materials science.[25] ^{19}F NMR spectroscopy has been used to investigate proteins, lipids, nucleic acids, and synthetic small-molecule ligands, as well as their complexes, both in solution[16,21] and in the solid state.[22–24] ^{19}F MAS NMR spectroscopy of biological systems remains underutilized owing to challenges associated with inherently broad lines due to strong homonuclear ^{19}F–^{19}F and heteronuclear ^{19}F–^{1}H dipolar couplings, particularly at traditionally used MAS frequencies below 25 kHz. Only three recent studies used faster spinning frequencies. In two of these studies, resolution enhancements were observed at 35 and 40 kHz,[14,26] whereas a report from our research group demonstrated that frequencies of 40–60 kHz yielded significant line narrowing for fluoro-substituted tryptophan solids, thus alleviating the need for ^{1}H decoupling.[27]

Here, we present a ^{19}F MAS NMR investigation of HIV-1 capsid protein tubular assemblies. Such tubes have been studied extensively by cryo-EM[28,29] and MAS NMR spectroscopy before,[1,30,31] and are excellent systems for exploring the potential of ^{19}F MAS NMR spectroscopy for the structural analysis of protein assemblies. HIV-1 capsid protein (CA) was uniformly labeled with 5-fluorotryptophan (5F-Trp). Trp residues are excellent sites for ^{19}F substitution, as this amino acid is generally rare in protein sequences and simple methodologies exist for introducing modified tryptophan residues into proteins by using standard *Escherichia coli* expression systems.[16,17] CA contains five tryptophan residues, four of which (W23, W80, W117, and W133) are located in the N-terminal domain (NTD), and one of which (W184) is located at the C-terminal (CTD) dimerization interface (Figure 1).

We show that fast MAS frequencies of 40–60 kHz result in narrow ^{19}F lines for CA assemblies, even in the absence of ^{1}H decoupling. Furthermore, by employing proton-driven spin

[*] M. Wang,[+] M. Lu,[+] M. P. Fritz, C. M. Quinn, T. Polenova
Department of Chemistry and Biochemistry, University of Delaware
Brown Laboratories, Newark, DE 19716 (USA)
E-mail: tpolenov@udel.edu
M. Wang,[+] M. Lu,[+] M. P. Fritz, I.-J. L. Byeon, C.-H. Byeon, A. M. Gronenborn, T. Polenova
Pittsburgh Center for HIV Protein Interactions
University of Pittsburgh School of Medicine
1051 Biomedical Science Tower 3, 3501 Fifth Avenue
Pittsburgh, PA 15261 (USA)
E-mail: amg100@pitt.edu
M. Lu,[+] I.-J. L. Byeon, C.-H. Byeon, A. M. Gronenborn
Department of Structural Biology
University of Pittsburgh School of Medicine
1051 Biomedical Science Tower 3, 3501 Fifth Avenue
Pittsburgh, PA 15261 (USA)
J. Struppe, W. Maas
Bruker Biospin Corporation
15 Fortune Drive, Billerica, MA (USA)
[+] These authors contributed equally.

Supporting information, including experimental methods, and the ORCID identification number(s) for the author(s) of this article can be found under: https://doi.org/10.1002/anie.201809060.

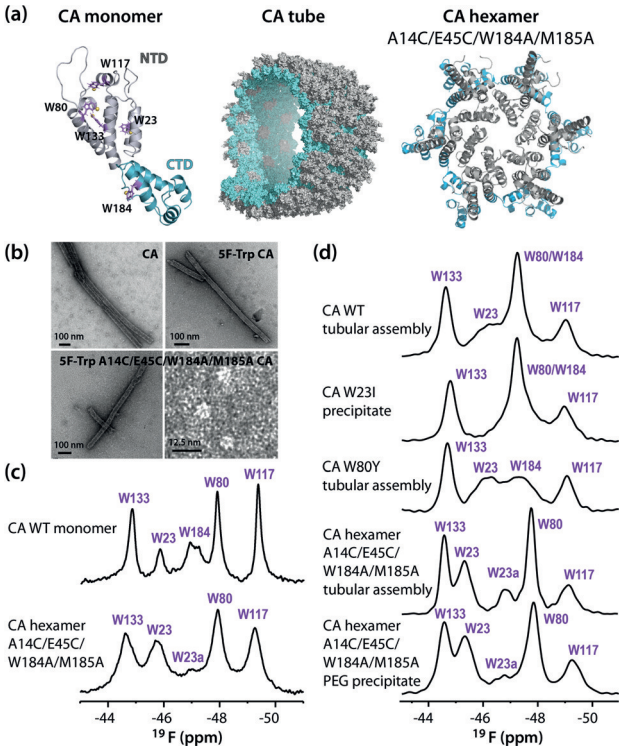

Figure 1. a) Structures of the HIV-1 CA monomer (W23, W80, W117, W133, and W184 are shown in purple stick representation with fluorine atoms as yellow spheres), a section of the CA tube, and the A14C/E45C/W184A/M185A CA cross-linked hexamer (NTD, gray; CTD, teal) b) Transmission electron micrographs of U-^{15}N CA tubes, 5F-Trp,U-^{15}N tubes, 5F-Trp,U-^{13}C,^{15}N A14C/E45C/W184A/M185A tubes, and 5F-Trp A14C/E45C/W184A/M185A CA soluble cross-linked hexamers. c) ^{19}F solution NMR spectra at 14.1 T of 5F-Trp,U-^{15}N CA and 5F-Trp,U-^{13}C,^{15}N A14C/E45C/W184A/M185A CA cross-linked hexamer. d) ^{19}F MAS NMR spectra (19.96 T; MAS frequency, 40 kHz) of (top to bottom): 5F-Trp,U-^{13}C,^{15}N CA tubes, 5F-Trp,U-^{15}N W23I mutant CA tubes, 5F-Trp,U-^{15}N W80Y mutant CA tubes, 5F-Trp,U-^{13}C,^{15}N A14C/E45C/W184A/M185A mutant CA tubes, and A14C/E45C/W184A/M185A cross-linked CA hexamer precipitated with PEG-4000.

diffusion (PDSD)[32] and/or radio-frequency-driven recoupling (RFDR),[33] it was possible to observe intramolecular ^{19}F–^{19}F correlations corresponding to distances of the order of 20 Å. To our knowledge, ^{19}F MAS NMR has not previously been applied to a very large protein assembly.

The replacement of all native tryptophan residues with 5F-Trp had no measurable effect on the in vitro tubular assemblies: The morphology and dimensions of U-^{15}N-CA and 5F-Trp,U-^{15}N CA tubes were indistinguishable from non-^{19}F-labeled tubes. (Figure 1b). Furthermore, no significant chemical shift perturbations (other than those associated with residues close to the substitution sites) were noted in the 2D ^{1}H-detected MAS (H)NH and (H)CH HETCOR spectra (see Figure S1 in the Supporting Information). Thus, the introduction of fluorine into CA does not interfere with assembly and does not perturb the overall structure of the tubes.

^{19}F chemical shifts are sensitive to the local environment. The ^{19}F solution NMR spectrum of unassembled CA (Figure 1c) exhibits several resonances of varying intensity, which were assigned by mutagenesis (see Figure S2). W80, W117, and W133 possess approximately unit intensity resonances at −47.9, −49.4, and −44.9 ppm, whereas W23 and W184 exhibit several smaller-intensity resonances at −45.9, −46.3, and −46.7 ppm and −48.1, −47.2, and −47.8 ppm, respectively. This observation is consistent with prior findings that W23 and W184 exists in several conformations in solution.[34] The multiple resonances of W184 arise from monomeric and different dimeric quaternary structures.[34] All ^{19}F chemical shifts are summarized in Table S1 of the Supporting Information.

Solid-state ^{19}F NMR spectra of CA tubular assemblies were acquired at MAS frequencies of 30, 40, and 60 kHz (Figure 1d; see also Figure S3). As can be appreciated by comparing the spectra at different frequencies (see Figure S3), for MAS frequencies below 60 kHz, proton decoupling is necessary to obtain sharp resonances. The ^{19}F line widths in the MAS NMR spectrum acquired at $\omega_r = 30$ kHz with high-power proton decoupling (0.5–1.3 ppm) are still broader than those in the spectrum recorded at $\omega_r = 60$ kHz without decoupling (0.3–1.0 ppm). The spectra collected at $\omega_r = 40$ kHz without decoupling exhibit line widths of 1.1 ppm. This observation is in agreement with our findings for fluoro-substituted tryptophan solids[27] and clearly illustrates the benefits of fast MAS conditions.

The general chemical shift range for all five 5F-Trp sidechain resonances is similar to that for CA in solution (−44.7 to −49.1 ppm), yet noticeable differences exist. Assemblies of several mutants were prepared, and in particular W23I, W80Y, and A14C/E45C/W184A/M185A samples permitted unambiguous assignments (Figure 1d). A14C/E45C/W184A/M185A was cross-linked into a hexamer, and the spectrum of this hexamer in the tubular assembly was very useful in this regard. The 5F-Trp resonances of W133 and W117 are at −44.7 and −49.1 ppm, respectively. W80 exhibits a relatively narrow resonance at −47.3 ppm, superimposed on the broad resonance of W184. W23 resonates at −46.3 ppm in the WT assembly and is shifted downfield to −45.3 ppm with the second, minor conformer at −46.8 ppm in the A14C/E45C/W184A/M185A hexamer mutant. The observed chemical shifts are summarized in Table 1 and in Table S2 of the Supporting Information. The W23 and W184 resonances are broader than the others and of the order of 1.3 ppm, suggesting some degree of conformational heterogeneity. However, in the tubular assembly of the hexamer, the W23 resonance at −45.3 ppm (major conformer) is narrower,

Table 1: MAS NMR experimental ^{19}F chemical-shift parameters for the 5F-Trp-substituted CA capsid tubular assemblies.

Field strength/ MAS frequency	Residue	δ_{iso} [ppm] (±0.1)	δ_{σ} [ppm] (±1.0)	η (±0.3)
19.96 T/ 15 kHz	W23	−46.3	44.4	0.4
	W80/W184	−47.3	46.1	0.0
	W117	−49.1	44.6	0.0
	W133	−44.7	45.3	0.3
11.74 T/ 4 kHz	W23	−46.1	44.6 (±1.6)	0.6
	W80/W184	−47.3	46.7	0.4
	W117	−49.1	44.1	0.4
	W133	−45.0	44.8	0.7

suggesting that conformational heterogeneity is reduced and a slightly different local environment is present.

The conformational heterogeneity observed for W184 at the CTD–CTD dimer interface comes as no surprise, since different side-chain conformers have been observed by X-ray crystallography (PDB 3NTE, 4XFX, 4XFY)[35,36] and NMR spectroscopy.[34] The side chain of W23 is buried in the NTD core and is essential for correct core assembly.[37] Solution NMR spectroscopy revealed multiple amide resonances for W23,[34] and its side chain was shown to be displaced by more than 3 Å in complexes of CA with potent antiviral capsid inhibitors, derivatives of benzodiazepines and benzoimidazoles,[38] indicative of side-chain conformational variability.

While isotropic chemical shifts are a key NMR observable, orientation-dependent chemical shift anisotropy (CSA) tensors are an even richer source of information for exploring local electronic and geometric structure. CSA parameters are also important for interfluorine distance measurements by spin-exchange experiments.[14] Furthermore, our long-term goal is to combine experiment and quantum-chemical calculations of ^{19}F CSA parameters in conjunction with ^{19}F–^{19}F distance restraints for the structure elucidation of large protein assemblies. While we have recently demonstrated the proof of principle on model crystalline tryptophans,[27] to apply this approach broadly it is necessary to establish a database of experimental ^{19}F CSA parameters for a range of proteins and protein assemblies. As the first step in this endeavor, we have determined experimental ^{19}F CSA parameters for HIV-1 capsid assemblies, a system that is well-established and extensively studied in our laboratories.

^{19}F CSA tensors for the WT CA tubular assemblies were recorded in two sets of experiments: i) at 11.74 T with a MAS frequency of 4 kHz and high-power ^{1}H decoupling, and ii) at 19.96 T with a MAS frequency of 15 kHz without ^{1}H decoupling. Good agreement for the ^{19}F CSA tensor parameters is obtained by both approaches (Figure 2; Table 1), with uncertainties of ± 1.0 ppm and ± 0.3 for the reduced anisotropy and the asymmetry parameters, respectively. We note that even at slow MAS frequencies, accurate CSA parameters can be obtained, even in the absence of ^{1}H decoupling, since no contribution from ^{19}F–^{19}F homonuclear dipolar interactions are present. Interestingly, no correlation between the magnitude of the reduced anisotropy and the isotropic chemical shift is observed.

Intra- and intermolecular ^{19}F–^{19}F distances in 5F-Trp-labeled CA assemblies are expected to range between 8.8 and 42.5 Å. Based on the X-ray structures of wild-type CA[36] and A14C/E45C/W184A/M185A CA cross-linked hexamers[39] (see Table S2), five pairs of Trp residues are separated by distances that are within a potentially accessible detection range in dipolar-based experiments: W80–W133 (8.8 Å), W117–W133 (9.8 Å), W80–117 (12.6 Å), W23–W133 (19.1 Å), and W23–W80 (23.1 Å). For fluorine distance measurements by MAS NMR spectroscopy, several methods are available: RFDR,[33] CODEX,[40] and, more recently, PDSD[32] and CORD.[41] In a recent study at 14.1 T which employed PDSD and CORD mixing at a MAS frequency of 25 kHz, correlations were observed for distances as long as 16 Å for long CORD mixing times of 306 ms.[14]

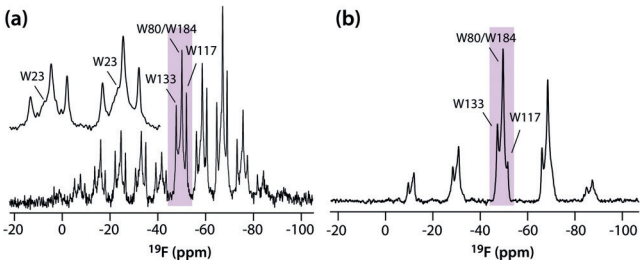

Figure 2. ^{19}F MAS NMR spectra of 5F-Trp,U-^{15}N CA tubes a) at 11.74 T and a MAS frequency of 4 kHz, and b) at 19.96 T and a MAS frequency of 15 kHz. The inset in (a) shows the W23 resonance.

In this study, for CA assemblies, we established that ideally MAS frequencies exceeding 35 kHz are required to ensure sufficiently narrow lines in the absence of ^{1}H decoupling (see Figure 1), an important consideration when using probes without separate ^{19}F and ^{1}H channels. MAS frequencies of 35, 40, and 60 kHz, and two mixing schemes—PDSD and RFDR, were used for detection of ^{19}F–^{19}F correlations in the fluorinated CA assemblies. These two sequences were selected on the basis of the following criteria: i) efficient polarization transfer over the full spectral width can be achieved; ii) no or minimal contributions from other anisotropic interactions are apparent; iii) insensitivity to experimental imperfections and off-resonance effects has been ascertained; and iv) RF powers compatible with the hardware can be applied.

PDSD spectra of fluorinated wild-type CA and cross-linked hexamer A14C/E45C/W184A/M185A CA assemblies, recorded at a MAS frequency of 35 kHz using a mixing time of 1 s (Figure 3 A,B), contain cross-peaks between W80 and W133 resonances, W80 and W117 resonances, and W23 and W133 resonances. The associated 5F positions are separated by 8.8, 12.6, and 19.1 Å, respectively. A W23–W80 cross-peak is also observed, corresponding to a F–F distance of 23.1 Å. Since PDSD is no longer an efficient mixing scheme for 40 and 60 kHz spinning frequencies at any practically attainable condition,[41] we employed RFDR mixing at these higher MAS frequencies. At both spinning frequencies, correlations between W80 and W133 as well as W80 and W117 resonances are observed with an RFDR mixing time of 8 ms (Figure 3). At 40 kHz, an additional cross-peak between W80 and W23 is present. At 60 kHz, the W133–W117 correlation appears, whereas the equivalent W117–W133 cross-peak is not seen. It is known that RFDR and other recoupling sequences may give rise to asymmetric cross-peak patterns, even when the magnetization is equal at the beginning of the recoupling period.[42] These asymmetric cross-peak patterns can be caused by multiple factors, such as different relaxation rates for individual sites during mixing.

^{19}F–^{19}F RFDR buildup curves were recorded for tubular assemblies of cross-linked A14C/E45C/W184A/M185A hexamer at a MAS frequency of 40 kHz (Figure 3 c). This assembly was used since W184 is not present and the resonance of W80 exhibits no overlap. Monitoring of the W80–W133 cross-peak intensity shows the polarization buildup (Figure 3 c), which did not reach maximum intensity even at a mixing time as long as 100 ms. Furthermore, it is highly unlikely that

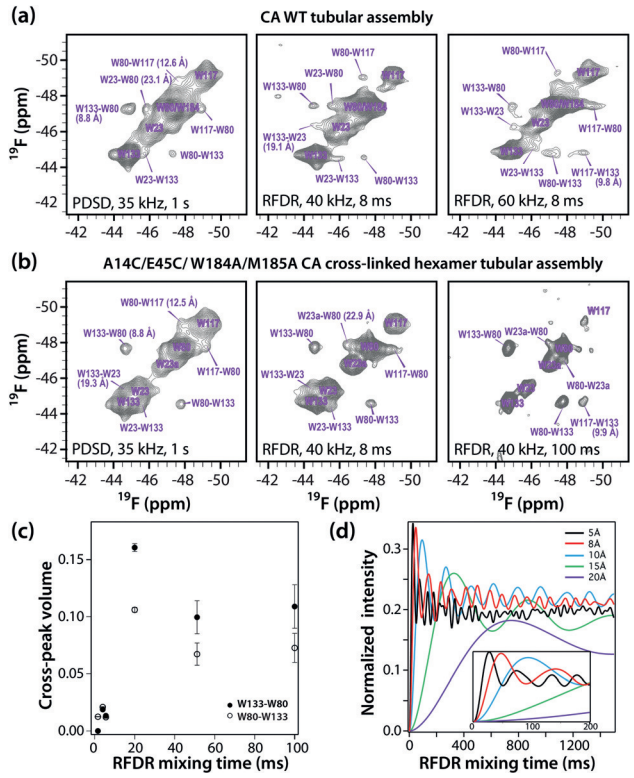

Figure 3. 2D ^{19}F–^{19}F correlation spectra (19.96 T) of a) 5F-Trp CA tubes and b) 5F-Trp A14C/E45C/W184A/M185A CA cross-linked hexamer tubes. MAS frequencies and mixing times in the ^{19}F–^{19}F RFDR spectra are listed. The first contour level was set to 5× noise rmsd. No ^{1}H decoupling was applied. c) Experimental ^{19}F–^{19}F RFDR buildup of the W80–W133 and W133–W80 cross-peak volumes in the 5F-Trp A14C/E45C/W184A/M185A CA cross-linked hexamer tubes (MAS frequency, 40 kHz). d) Simulated ^{19}F–^{19}F RFDR cross-peak buildup curves for ^{19}F–^{19}F distances of 5–20 Å (simulation parameters are provided in the Supporting Information). The inset is an expansion for up to 200 ms.

intermolecular contacts compromise the measurements for the two assemblies under investigation, as the shortest intermolecular ^{19}F–^{19}F distance is 21.7 Å between W80 and W117. In other proteins and protein assemblies, intermolecular ^{19}F–^{19}F distances may be short enough to contribute to RFDR polarization transfer. In such cases isotopic dilution can be used to distinguish between intra- and intermolecular correlations.

The simulated RFDR buildup curves for MAS frequencies of 20, 40, and 60 kHz and ^{19}F–^{19}F distances ranging from 5 to 20 Å are shown in Figure 3d and Figure S5 in the Supporting Information. We note that quantitative comparisons with the experimental buildup rates are not possible, as the SIMPSON simulations do not include relaxation. Nevertheless, excellent qualitative agreement between the experimental and calculated buildup curves is noted, and it appears that for correlations corresponding to 15–20 Å distances, long mixing times of the order of hundreds of milliseconds are necessary.

Overall, the results of this study highlight the potential of ^{19}F MAS NMR spectroscopy for analyzing structural properties and interactions of HIV-1 capsid. To our knowledge, this investigation is the first of its kind on a large protein assembly. The chemical shift dispersion is high, with separation of at least three of the five resonances (W80, W117, and W133). For two tryptophan residues, W23 and W184, multiple resonances are present, indicating conformational heterogeneity, previously also observed in solution.

One important outcome of the current investigation is that at fast MAS conditions (frequencies of 40–60 kHz), the lines are sufficiently narrow, obviating the need for decoupling. Under these fast MAS conditions, nanometer-range interfluorine distance restraints can be extracted from PDSD and RFDR experiments.

Taken together, our results open up exciting and far-reaching possibilities for the widespread use of ^{19}F fast MAS, including the characterization of proteins and protein assemblies, without requiring specialized probes capable of simultaneous ^{19}F and ^{1}H radiofrequency irradiation. We envision that ultrafast MAS (> 100 kHz) conditions will further benefit resolution and enable ^{19}F MAS NMR spectroscopy on a wide range of large biological systems.

Acknowledgements

We thank Mike Delk (University of Pittsburgh) for solution NMR technical support, and Guangjin Hou (University of Delaware, currently at the Institute of Chemical Physics, Dalian, China) for help with several MAS NMR experiments. This research was supported by the National Science Foundation (NSF Grant CHE-1708773 to A.M.G. and T.P.) and by the National Institutes of Health (NIGMS and NIAID, Grant P50 GM082251, Technology Development Project on MAS NMR). We acknowledge the National Science Foundation (NSF grant CHE-0959496) for the acquisition of the 850 MHz NMR spectrometer at the University of Delaware, and the National Institutes of Health (NIH Grants P30GM103519 and P30GM110758) for the support of core instrumentation infrastructure at the University of Delaware.

Conflict of interest

The authors declare no conflict of interest.

Keywords: capsids · ^{19}F NMR spectroscopy · magic angle spinning · protein assemblies · protein structures

How to cite: *Angew. Chem. Int. Ed.* **2018**, *57*, 16375–16379
Angew. Chem. **2018**, *130*, 16613–16617

[1] C. M. Quinn, T. Polenova, *Q. Rev. Biophys.* **2017**, *50*, e1.
[2] A. Loquet, N. El Mammeri, J. Stanek, M. Berbon, B. Bardiaux, G. Pintacuda, B. Habenstein, *Methods* **2018**, *138–139*, 26–38.
[3] D. Aucoin, D. Camenares, X. Zhao, J. Jung, T. Sato, S. O. Smith, *J. Magn. Reson.* **2009**, *197*, 77–86.
[4] R. Linser, B. Bardiaux, V. Higman, U. Fink, B. Reif, *J. Am. Chem. Soc.* **2011**, *133*, 5905–5912.
[5] J. S. Retel, A. J. Nieuwkoop, M. Hiller, V. A. Higman, E. Barbet-Massin, J. Stanek, L. B. Andreas, W. T. Franks, B. J. van Rossum, K. R. Vinothkumar, L. Handel, G. G. de Palma, B. Bardiaux, G.

Pintacuda, L. Emsley, W. Kuhlbrandt, H. Oschkinat, *Nat. Commun.* **2017**, *8*, 2073.
[6] M. T. Colvin, R. Silvers, Q. Z. Ni, T. V. Can, I. Sergeyev, M. Rosay, K. J. Donovan, B. Michael, J. Wall, S. Linse, R. G. Griffin, *J. Am. Chem. Soc.* **2016**, *138*, 9663 – 9674.
[7] M. D. Tuttle, G. Comellas, A. J. Nieuwkoop, D. J. Covell, D. A. Berthold, K. D. Kloepper, J. M. Courtney, J. K. Kim, A. M. Barclay, A. Kendall, W. Wan, G. Stubbs, C. D. Schwieters, V. M. Lee, J. M. George, C. M. Rienstra, *Nat. Struct. Mol. Biol.* **2016**, *23*, 409 – 415.
[8] C. Shi, P. Fricke, L. Lin, V. Chevelkov, M. Wegstroth, K. Giller, S. Becker, M. Thanbichler, A. Lange, *Sci. Adv.* **2015**, *1*, e1501087.
[9] S. Yan, C. Guo, G. Hou, H. Zhang, X. Lu, J. C. Williams, T. Polenova, *Proc. Natl. Acad. Sci. USA* **2015**, *112*, 14611 – 14616.
[10] L. He, B. Bardiaux, M. Ahmed, J. Spehr, R. Konig, H. Lunsdorf, U. Rand, T. Luhrs, C. Ritter, *Proc. Natl. Acad. Sci. USA* **2016**, *113*, E272 – 281.
[11] S. Wang, R. A. Munro, L. Shi, I. Kawamura, T. Okitsu, A. Wada, S. Y. Kim, K. H. Jung, L. S. Brown, V. Ladizhansky, *Nat. Methods* **2013**, *10*, 1007 – 1012.
[12] S. G. Zech, A. J. Wand, A. E. McDermott, *J. Am. Chem. Soc.* **2005**, *127*, 8618 – 8626.
[13] M. L. Gilchrist, K. Monde, Y. Tomita, T. Iwashita, K. Nakanishi, A. E. McDermott, *J. Magn. Reson.* **2001**, *152*, 1 – 6.
[14] M. Roos, T. Wang, A. A. Shcherbakov, M. Hong, *J. Phys. Chem. B* **2018**, *122*, 2900 – 2911.
[15] Y. G. Gakh, A. A. Gakh, A. M. Gronenborn, *Magn. Reson. Chem.* **2000**, *38*, 551 – 558.
[16] N. G. Sharaf, A. M. Gronenborn in *Isotope Labeling of Biomolecules—Labeling Methods*, *Vol. 565* (Ed.: Z. Kelman), Elsevier Academic Press, San Diego, **2015**, pp. 67 – 95.
[17] P. B. Crowley, C. Kyne, W. B. Monteith, *Chem. Commun.* **2012**, *48*, 10681 – 10683.
[18] R. Campos-Olivas, R. Aziz, G. L. Helms, J. N. S. Evans, A. M. Gronenborn, *FEBS Lett.* **2002**, *517*, 55 – 60.
[19] M. N. Asada, T. Nemoto, H. Mimura, *J. Pharm. Sci.* **2016**, *105*, 1233 – 1238.
[20] F. Zhang, Q. Zhou, G. Yang, L. An, F. Li, J. Wang, *Chem. Commun.* **2018**, *54*, 3879 – 3882.
[21] J. L. Kitevski-LeBlanc, R. S. Prosser, *Prog. Nucl. Magn. Reson. Spectrosc.* **2012**, *62*, 1 – 33.
[22] K. Koch, S. Afonin, M. Ieronimo, M. Berditsch, A. S. Ulrich in *Solid State NMR*, *Vol. 306* (Ed.: J. C. C. Chan), Springer, Heidelberg, **2012**, pp. 89 – 118.
[23] J. K. Williams, D. Tietze, M. Lee, J. Wang, M. Hong, *J. Am. Chem. Soc.* **2016**, *138*, 8143 – 8155.
[24] U. A. Hellmich, N. Pfleger, C. Glaubitz, *Photochem. Photobiol.* **2009**, *85*, 535 – 539.
[25] K. P. Nartowski, D. Malhotra, L. E. Hawarden, J. Sibik, D. Iuga, J. A. Zeitler, L. Fábián, Y. Z. Khimyak, *Angew. Chem.* **2016**, *128*, 9050 – 9054.
[26] A. A. Shcherbakov, M. Hong, *J. Biomol. NMR* **2018**, *71*, 31 – 43.
[27] M. Lu, S. Sarkar, M. Wang, J. Kraus, M. Fritz, C. M. Quinn, S. Bai, S. T. Holmes, C. Dybowski, G. P. A. Yap, J. Struppe, I. V. Sergeyev, W. Maas, A. M. Gronenborn, T. Polenova, *J. Phys. Chem. B* **2018**, *122*, 6148 – 6155.
[28] M. Wang, C. M. Quinn, J. R. Perilla, H. Zhang, R. Shirra, Jr., G. Hou, I. J. Byeon, C. L. Suiter, S. Ablan, E. Urano, T. J. Nitz, C. Aiken, E. O. Freed, P. Zhang, K. Schulten, A. M. Gronenborn, T. Polenova, *Nat. Commun.* **2017**, *8*, 1779.
[29] P. Zhang, X. Meng, G. Zhao, *Methods Mol. Biol.* **2013**, *955*, 381 – 399.
[30] C. M. Quinn, M. Lu, C. L. Suiter, G. Hou, H. Zhang, T. Polenova, *Prog. Nucl. Magn. Reson. Spectrosc.* **2015**, *86 – 87*, 21 – 40.
[31] M. J. Bayro, B. Chen, W. M. Yau, R. Tycko, *J. Mol. Biol.* **2014**, *426*, 1109 – 1127.
[32] N. Bloembergen, *Physica* **1949**, *15*, 386 – 426.
[33] A. E. Bennett, C. M. Rienstra, J. M. Griffiths, W. Zhen, P. T. J. Lansbury, R. G. Griffin, *J. Chem. Phys.* **1998**, *108*, 9463 – 9479.
[34] I. J. L. Byeon, G. J. Hou, Y. Han, C. L. Suiter, J. Ahn, J. Jung, C. H. Byeon, A. M. Gronenborn, T. Polenova, *J. Am. Chem. Soc.* **2012**, *134*, 6455 – 6466.
[35] S. Du, L. Betts, R. Yang, H. Shi, J. Concel, J. Ahn, C. Aiken, P. Zhang, J. I. Yeh, *J. Mol. Biol.* **2011**, *406*, 371 – 386.
[36] A. T. Gres, K. A. Kirby, V. N. KewalRamani, J. J. Tanner, O. Pornillos, S. G. Sarafianos, *Science* **2015**, *349*, 99 – 103.
[37] S. Tang, T. Murakami, B. E. Agresta, S. Campbell, E. O. Freed, J. G. Levin, *J. Virol.* **2001**, *75*, 9357 – 9366.
[38] C. T. Lemke, S. Titolo, U. von Schwedler, N. Goudreau, J. F. Mercier, E. Wardrop, A. M. Faucher, R. Coulombe, S. S. Banik, L. Fader, A. Gagnon, S. H. Kawai, J. Rancourt, M. Tremblay, C. Yoakim, B. Simoneau, J. Archambault, W. I. Sundquist, S. W. Mason, *J. Virol.* **2012**, *86*, 6643 – 6655.
[39] O. Pornillos, B. K. Ganser-Pornillos, S. Banumathi, Y. Hua, M. Yeager, *J. Mol. Biol.* **2010**, *401*, 985 – 995.
[40] E. R. deAzevedo, W. G. Hu, T. J. Bonagamba, K. Schmidt-Rohr, *J. Am. Chem. Soc.* **1999**, *121*, 8411 – 8412.
[41] G. Hou, S. Yan, J. Trebosc, J. P. Amoureux, T. Polenova, *J. Magn. Reson.* **2013**, *232*, 18 – 30.
[42] K.-Y. Huang, A. B. Siemer, A. E. McDermott, *J. Magn. Reson.* **2011**, *208*, 122 – 127.

Manuscript received: August 6, 2018
Accepted manuscript online: September 17, 2018
Version of record online: October 19, 2018

